

See discussions, stats, and author profiles for this publication at: <https://www.researchgate.net/publication/228008707>

Evaluation of various DFT protocols for computing ^1H and ^{13}C chemical shifts to distinguish stereoisomers: Diastereomeric 2-, 3-, and 4-methylcyclohexanols as a test set

ARTICLE in JOURNAL OF PHYSICAL ORGANIC CHEMISTRY · MAY 2007

Impact Factor: 1.38 · DOI: 10.1002/poc.1151

CITATIONS

15

READS

3

5 AUTHORS, INCLUDING:



Ziyad F Al-Rashid

Alcohol Research Group

12 PUBLICATIONS 239 CITATIONS

SEE PROFILE



Christopher J Cramer

University of Minnesota Twin Cities

531 PUBLICATIONS 23,105 CITATIONS

SEE PROFILE

Evaluation of various DFT protocols for computing ^1H and ^{13}C chemical shifts to distinguish stereoisomers: diastereomeric 2-, 3-, and 4-methylcyclohexanols as a test set

Keith W. Wiitala, Ziyad F. Al-Rashid, Vadims Dvornikovs, Thomas R. Hoye* and Christopher J. Cramer*

Department of Chemistry and Supercomputing Institute, University of Minnesota, 207 Pleasant St. SE, Minneapolis, Minnesota 55455-0431, USA

Received 14 December 2006; accepted 16 December 2006



ABSTRACT: ^1H and ^{13}C NMR chemical shifts were measured for a set of six isomers—the *cis* and *trans* 2-, 3-, and 4-methylcyclohexanols. ^1H and ^{13}C NMR chemical shifts were computed at the B3LYP, WP04, WC04, and PBE1 density functional levels for the same compounds, taking into account the Boltzmann distribution among conformational isomers (chair–chair forms and hydroxyl rotamers). The experimental *versus* computed chemical shift values for proton and carbon were compared and evaluated (using linear correlation (r^2), total absolute error ($|\Delta\delta|_T$), and mean unsigned error (MUE) criteria) with respect to the relative ability of each method to distinguish between *cis* and *trans* stereoisomers for each of the three constitutional isomers. For ^{13}C shift data, results from the B3LYP and PBE1 density functionals were not sufficiently accurate to distinguish all three pairs of stereoisomers, while results using the WC04 functional did do so. For ^1H shift data, each of the WP04, B3LYP, and PBE1 methods was sufficiently accurate to make the proper stereochemical distinction for each of the three pairs. Applying a linear correction to the computed data improved both the absolute accuracy and the degree of discrimination for most of the methods. The nature of the cavity definition used for continuum solvation had little effect. Overall, use of proton chemical shift data was more discriminating than use of carbon data. Copyright © 2007 John Wiley & Sons, Ltd.

Supplementary electronic material for this paper is available in Wiley InterScience at <http://www.mrw.interscience.wiley.com/suppmat/0894-3230/suppmat/v20.html>

KEYWORDS: NMR; density functional theory

INTRODUCTION

Stereochemical features influence the properties of organic molecules, often in quite important ways (e.g., biological activity). The identification of stereocenters and the assignment of their relative and absolute configurations is a key step in the structure determination of new compounds, whether natural (e.g., newly identified natural-products) or synthetic (e.g., product(s) of a reaction in a target-driven synthetic approach to a natural product or a drug candidate).

Because stereochemistry influences the local environment about magnetically active nuclei, nuclear magnetic resonance (NMR) can be a useful technique for the assignment of configuration of stereocenters. However, differences in chemical shifts (and coupling constants)

among various stereoisomers can be small and are not always easily rationalized. Moreover, in most instances spectra are not available for the set of all possible stereoisomers. In the absence of having an opportunity to make comparisons between the spectra of any pair of diastereomers, it is often a challenge to assign relative configuration based solely on analysis of the NMR spectra (typically, ^1H and ^{13}C) of the single isomer in hand.

Comparison, when available, of NMR data for a new compound with that from a close structural relative is often very valuable. This simple concept was a major driving principle behind the development of Kishi's powerful 'universal NMR database' approach for assignment of stereostructure to complex molecules.¹ This protocol, however, requires the synthesis of libraries of diastereomeric compounds and is, therefore, limited to compound classes that have a ubiquitous constitution.

Quantum mechanical calculations permit the prediction of NMR chemical shifts, and the use of such computations to support the interpretation and assignment of NMR spectra has grown in recent years.² Such an

*Correspondence to: Thomas R. Hoye or Christopher J. Cramer, Department of Chemistry and Supercomputing Institute, University of Minnesota, 207 Pleasant St. SE, Minneapolis, Minnesota 55455-0431, USA.
E-mail: hoye@chem.umn.edu

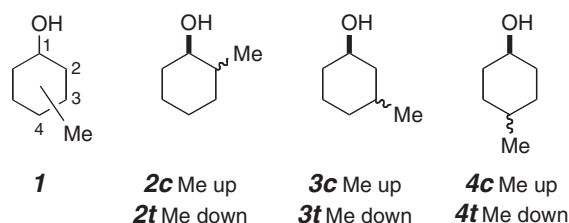


Figure 1. The isomeric *cis* (**c**) and *trans* (**t**) methylcyclohexanols investigated in this study

approach is attractive since it is inherently unlimited in the constitutional setting in which it is applied. For small to medium-sized molecules (those having molecular weights of ~100–500) density functional theory (DFT) is the quantum mechanical method that best combines efficiency with computational accuracy.³ Comparison of DFT predictions to experimental NMR data has in several instances facilitated assignment of structure and relative stereochemical configurations.⁴

In a prior paper,⁵ we reported the design of the WP04 and WC04 density functionals, which were developed specifically for the accurate prediction of ¹H and ¹³C chemical shifts, respectively, of organic molecules in deuteriochloroform. A training set of ~40 simple, common organic compounds was used to guide the development of those functionals. We also briefly summarized measured and computed ¹H and ¹³C chemical-shift profiles for a set of methylated cyclohexanols **1**, namely the *cis*- and *trans*-2-, 3-, and 4-methylcyclohexanols (six isomers total, **2c/t–4c/t**, Fig. 1). However, that earlier report did not include a study of the relative ability of *different* functionals to distinguish between pairs of *cis*- and *trans*-stereoisomers in this series. We chose the series of methylated cyclohexanols as a test set for this purpose because they are conformationally tractable, have relatively small shift differences between the *cis* and *trans* stereoisomers, and incorporate substructural elements that are related, by extrapolation, to a wide variety of molecules. Below we provide a complete analysis of the utility of various theoretical models (including some not previously assessed in Ref. [5]) for the assignment of stereochemistry in **2–4**.

COMPUTATIONAL METHODS

Each methylcyclohexanol was modeled as a family of conformers characterized by different dihedral angles about the C—O bond (to generate hydroxy rotamers) and different chair forms. The six conformers for *cis*-2-methylcyclohexanol (**2c**) are illustrated in Fig. 2. Conformer geometries were fully optimized at the density functional level of theory employing the hybrid generalized gradient approximation (GGA) functional B3LYP⁶ and the 6-31G(d) basis set.⁷ Chloroform solvation effects were always used via the integral equation formalism polarized continuum model (IEFPCM).⁸ Substrate

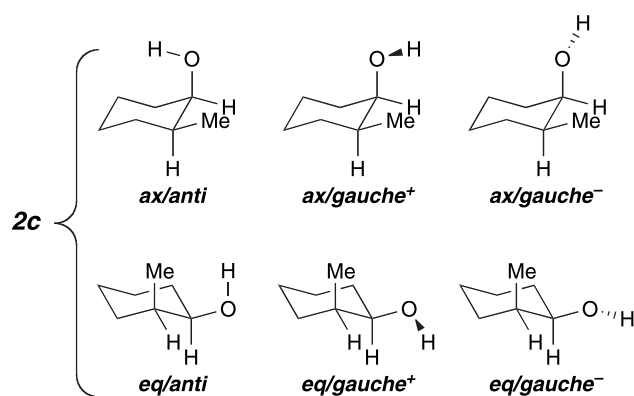


Figure 2. Conformer family used to model *cis*-2-methylcyclohexanol (**2c**)

solvation cavities were generated using either united-atom radii⁹ (UA0) or individual atomic radii (using the values of Bondi)¹⁰ and their effects compared.

For each optimized geometry, ¹H and ¹³C chemical shifts relative to TMS were computed using the gauge including atomic orbitals (GIAO) formalism and the basis set 6-311+G(2d,p). We examined four hybrid generalized gradient approximation functionals, namely, B3LYP, WP04,⁵ WC04,⁵ and PBE1.¹¹ Population-averaged chemical shifts for each family of conformers were computed assuming Boltzmann statistics using B3LYP/6-311+G(2d,p) free energies including IEFPCM chloroform solvation effects computed with Bondi-radii derived cavities unless specified otherwise (note that WP04 and WC04 were designed for chemical-shift predictions, and *not* for accurate energetic predictions). A pruned (75 302) integration grid containing 75 radial shells and 302 angular points per shell (approximately 7000 points for each atom) was used throughout the study. Density functional calculations were carried out using the Gaussian 03 suite of electronic structure programs.¹²

RESULTS AND DISCUSSION

Assigning relative configuration

Because of their semi-rigid nature and well-defined equilibria,¹³ we considered the methylcyclohexanols **2c/t–4c/t** (Fig. 3) to be ideal for evaluating the utility of different DFT protocols for making stereochemical assignments. Moreover, the relatively small differences between chemical shifts of analogous atoms in different stereoisomers was judged to pose a significant challenge for using agreement between theory and experiment as an assignment protocol.

Structures **2c/t–4c/t** are subject to chair–chair inter-conversion equilibria (Fig. 3) that, in addition to hydroxyl rotameric equilibria (cf. Fig. 2), were accounted for through Boltzmann-averaging of computed chemical shifts using computed energies. For each conformer, the computed ¹H chemical shift for the protons of its methyl

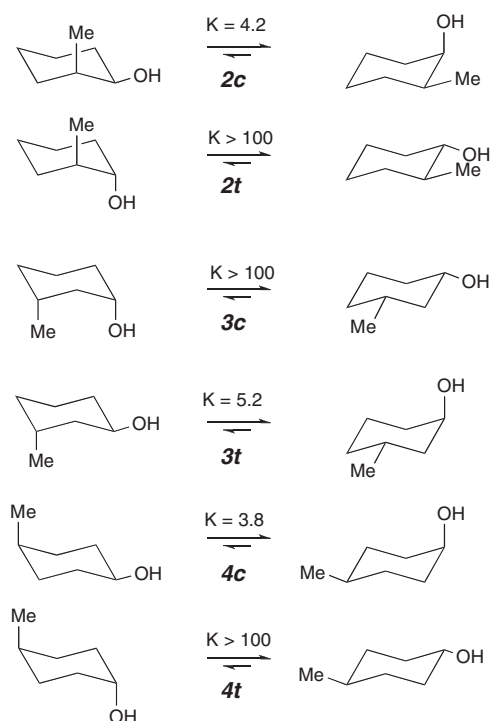


Figure 3. Each monomethylcyclohexanol (**2c/t** through **4c/t**) was modeled by a family of six conformers (cf. hydroxyl rotamers in Figure 2). The indicated equilibrium constants arise from Boltzmann-averaging (at 298 K) of the IEFPCM/B3LYP/6-311+G(2d,p)//IEFPCM/B3LYP/6-31G(d) computed energy of each of the three hydroxyl rotamers for each of the two different chair conformations

group were averaged arithmetically to reflect their equivalence owing to free rotation of that group at 298 K. Twist-boat conformers were also located at the IEFPCM/B3LYP/6-31G(d) level. Their relative energies were never less than 5.1 kcal/mol above the global minimum, however, and on that basis they were not included in the Boltzmann average.

The utility of the computed chemical shifts for distinguishing between relative configurations of stereoisomeric methylcyclohexanols was quantified based on correlation coefficients (r^2) deriving from linear regression of computed chemical shifts on experimental values and also the total absolute error between theoretical and experimental chemical shifts ($|\Delta\delta|_T$) for all of the atoms evaluated [7 carbon atoms, 13 hydrogen atoms (OH not done)]. Calculated mean unsigned error (MUE) values were also used to compare the per atom performance of the various methods employed.

In Tables 1–3, the correlation matrices between theoretical and experimental hydrogen chemical shifts are shown for the three pairs of stereoisomers (there is little ambiguity in assigning constitutional isomers and we do not discuss this point further). As the data presented in Table 1 indicate, for all stereochemical pairs, the B3LYP method (with chloroform solvation effects included) was able convincingly to distinguish relative configuration (i.e., *cis*- vs. *trans*-) for all three pairs of diastereomers. Consider the comparison data in Table 1 for **2c**, namely, the experimental shift data for **2c** ($2c^{\text{exp}}$) versus the computed shifts for each of **2c** and **2t** ($2c^{\text{comp}}$ and $2t^{\text{comp}}$). The first row of data shows the correlation coefficient (r^2) for the comparison of the 13 protons (which is excellent for the matched pair); the second row lists the total absolute error (~ 6 times larger for the mismatched); the third row shows the MUE (which is simply the second row entry divided by 13) and indicates the magnitude of the chemical shift error per proton. The data for all entries in all the Tables are presented in this format. The correlation coefficient comparisons strongly favor the matched set for all six of the methylcyclohexanols. Likewise, the mean total absolute error (as well as MUE) comparisons also consistently favor the matched pair and to a remarkably similar extent (i.e., by a factor of ~ 6 –8) for all three diastereomeric pairs. This B3LYP

Table 1. Correlation matrices between IEFPCM/B3LYP/6-311+G(2d,p)//IEFPCM/B3LYP/6-31G(d) and experimental ^1H NMR chemical shifts^a

	$2c^{\text{comp}}$	$2t^{\text{comp}}$		$3c^{\text{comp}}$	$3t^{\text{comp}}$		$4c^{\text{comp}}$	$4t^{\text{comp}}$
$2c^{\text{exp}}$	0.9971	0.8334	$3c^{\text{exp}}$	0.9950	0.8763	$4c^{\text{exp}}$	0.9993	0.8335
	<i>0.54</i> (0.04)	<i>3.03</i> (0.23)		<i>0.66</i> (0.05)	<i>3.45</i> (0.26)		<i>0.42</i> (0.03)	<i>3.24</i> (0.25)
$2t^{\text{exp}}$	0.8167	0.9957	$3t^{\text{exp}}$	0.8856	0.9990	$4t^{\text{exp}}$	0.8744	0.9983
	<i>3.55</i> (0.27)	<i>0.48</i> (0.04)		<i>3.15</i> (0.24)	<i>0.44</i> (0.03)		<i>3.03</i> (0.23)	<i>0.52</i> (0.04)

^a Data are reported as r^2 (unitless), $|\Delta\delta|_T$ (ppm, italic), and MUE (ppm, parentheses).

Table 2. Correlation matrices between IEFPCM/WP04/6-311+G(2d,p)//IEFPCM/B3LYP/6-31G(d) and experimental ^1H NMR chemical shifts^a

	$2c^{\text{comp}}$	$2t^{\text{comp}}$		$3c^{\text{comp}}$	$3t^{\text{comp}}$		$4c^{\text{comp}}$	$4t^{\text{comp}}$
$2c^{\text{exp}}$	0.9985	0.9050	$3c^{\text{exp}}$	0.9899	0.8717	$4c^{\text{exp}}$	0.9975	0.9279
	<i>0.70</i> (0.05)	<i>2.54</i> (0.20)		<i>1.09</i> (0.08)	<i>3.35</i> (0.26)		<i>1.18</i> (0.09)	<i>2.79</i> (0.21)
$2t^{\text{exp}}$	0.8098	0.9843	$3t^{\text{exp}}$	0.9310	0.9979	$4t^{\text{exp}}$	0.8675	0.9938
	<i>3.42</i> (0.26)	<i>0.95</i> (0.07)		<i>2.83</i> (0.22)	<i>1.04</i> (0.08)		<i>3.00</i> (0.23)	<i>1.05</i> (0.08)

^a Data are reported as r^2 (unitless), $|\Delta\delta|_T$ (ppm, italic), and MUE (ppm, parentheses).

Table 3. Correlation matrices between IEFPCM/PBE1/6-311+G(2d,p)//IEFPCM/B3LYP/6-31G(d) and experimental ^1H NMR chemical shifts^a

	2c^{comp}	2t^{comp}		3c^{comp}	3t^{comp}		4c^{comp}	4t^{comp}
2c^{exp}	0.9977 0.50 (0.04)	0.8332 3.11 (0.24)	3c^{exp}	0.9951 0.91 (0.07)	0.8789 3.37 (0.26)	4c^{exp}	0.9996 0.78 (0.06)	0.9004 3.17 (0.24)
2t^{exp}	0.8190 3.49 (0.27)	0.9967 0.68 (0.05)	3t^{exp}	0.8839 3.41 (0.26)	0.9992 0.76 (0.06)	4t^{exp}	0.8782 3.03 (0.23)	0.9958 1.01 (0.08)

^aData are reported as r^2 (unitless), $|\Delta\delta|_{\text{T}}$ (ppm, italic), and MUE (ppm, parentheses).

method had an average difference between theory and experiment for the matched *versus* the mismatched pairings of 0.1441 units for r^2 and 2.73 ppm for the total absolute error $|\Delta\delta|_{\text{T}}$.

Comparisons of computed and experimental ^1H shifts, and the linear regressions of the former on the latter for different relative configurations, are illustrated in Fig. 4 for the $2\text{c}/\text{t}$ pair at the IEFPCM/B3LYP/6-311+G(2d,p)//IEFPCM/B3LYP/6-31G(d) level (Table 1 data). The better linear relationships associated with the correct stereochemical pairings are evident from visual inspection, and also from the slopes and intercepts of the best-fit lines, which should ideally be exactly 1 and 0, respectively.

Similarly in Tables 2 and 3, the WP04 and PBE1 methods (including chloroform solvation effects) were also able to convincingly distinguish relative configuration within all three stereochemical pairs. WP04 had an average difference between theory and experiment of

0.1082 units for r^2 and 1.99 ppm for the total absolute error $|\Delta\delta|_{\text{T}}$, while PBE1 yielded values of 0.1318 units and 2.49 ppm, respectively. Each of the three methods employed for computing ^1H chemical shifts was decisive in its ability to distinguish between pairs of stereoisomers. Plots similar to Fig. 4 can be generated in each case, but in the interests of brevity we do not present them here.

Even though each method used for computing ^1H shifts did an excellent job of distinguishing stereoisomeric pairs, such was not the case for the various methods we studied for ^{13}C chemical shifts. In particular, computations using either the B3LYP or the PBE1 method were inadequate. For example, as shown in Table 4 (for B3LYP), although the r^2 values for comparison of the experimental data for 2t (2t^{exp}) *versus* the computed shifts for each of 2c and 2t (2c^{comp} and 2t^{comp}) indicate a better fit for the correct stereoisomeric pairings, the total absolute error criterion ($|\Delta\delta|_{\text{T}}$) leads to an incorrect prediction. In the comparison of the experimental data for

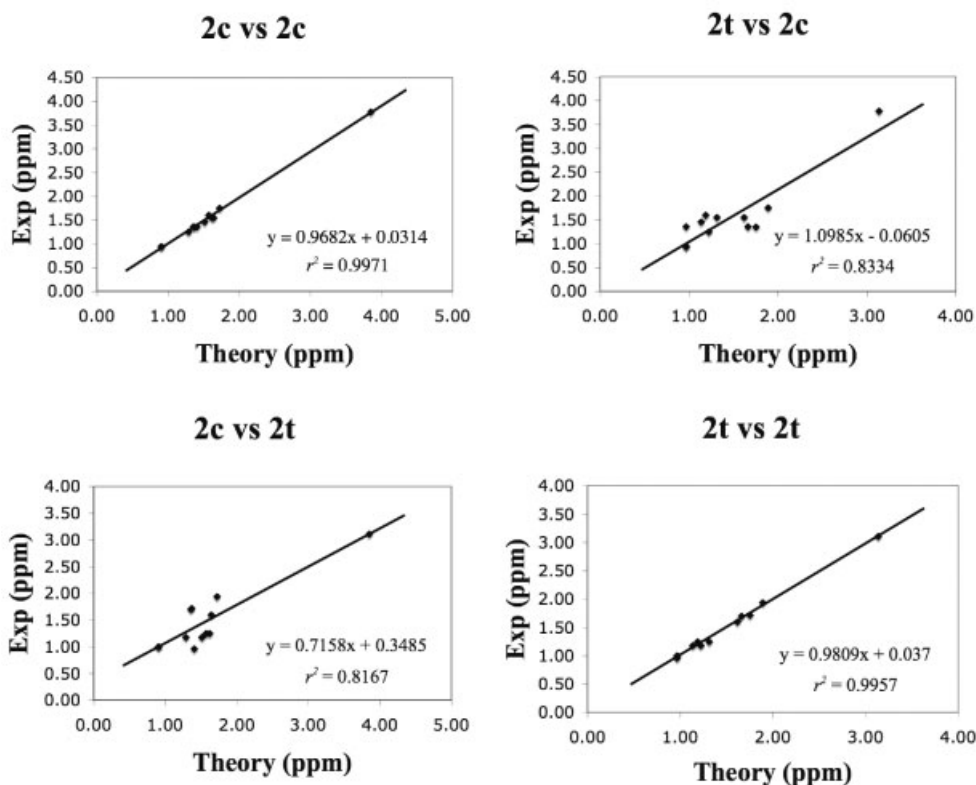
**Figure 4.** An example (2c vs. 2t) of a regression comparison of theoretical and experimental ^1H chemical shift data that form the basis for the statistics in Table 1

Table 4. Correlation matrices between IEFPCM/B3LYP/6-311+G(2d,p)//IEFPCM/B3LYP/6-31G(d) and experimental ^{13}C NMR chemical shifts^a

	2c^{comp}	2t^{comp}		3c^{comp}	3t^{comp}		4c^{comp}	4t^{comp}
2c^{exp}	0.9958 33.2 (4.7)	0.9875 57.8 (8.3)	3c^{exp}	0.9933 33.4 (4.8)	0.9943 15.4 (2.2)	4c^{exp}	0.9931 33.1 (4.7)	0.9831 53.1 (7.6)
2t^{exp}	0.9928 10.7 (1.5)	0.9953 33.4 (4.8)	3t^{exp}	0.9658 51.5 (7.4)	0.9917 33.5 (4.8)	4t^{exp}	0.9809 13.8 (2.0)	0.9936 33.3 (4.8)

^a Data are reported as r^2 (unitless), $|\Delta\delta|_{\text{T}}$ (ppm, italic), and MUE (ppm, parentheses).

3c (**3c^{exp}**) versus the computed **3c^{comp}** and **3t^{comp}** values, both the r^2 and $|\Delta\delta|_{\text{T}}$ criteria lead to an incorrect prediction. Similarly, in the comparison of the experimental data for **4t** (**4t^{exp}**) versus the computed **4c^{comp}** and **4t^{comp}** values, both the r^2 and $|\Delta\delta|_{\text{T}}$ criteria lead to an incorrect prediction. As shown in Table 5, ^{13}C chemical shifts computed at the PBE1 level also failed to distinguish unambiguously between some of the stereoisomeric pairs.

Given the failure of the B3LYP or the PBE1 methods, we next examined the performance of our WC04 functional, which was specifically developed for the purpose of computing ^{13}C shifts with greater accuracy.⁵ As shown in Table 6, the WC04 method is indeed able to differentiate all of the methylcyclohexanol stereoisomeric pairs convincingly with an average difference of 0.0100 units for r^2 and 9.8 ppm for the total absolute error $|\Delta\delta|_{\text{T}}$. Figure 5 illustrates the regressions summarized in Table 6 for the **2c/t** pair.

Linear correction of computed chemical shifts

Linear corrections of computed chemical shifts have been found to be useful for correcting systematic errors associated with particular density functionals to improve

accuracy.^{4h,5,14} The utility of these corrections was examined here with respect to improving the stereochemical distinctions in the stereoisomeric methylcyclohexanol pairs. In particular, the linear corrections listed in Table 7 were applied to raw ^1H and ^{13}C chemical shift values (δ^{comp}) obtained with each of the functionals we studied; corrected predictions (δ^{corr}) were determined according to:

$$\delta^{\text{corr}} = m \cdot \delta^{\text{comp}} + b \quad (1)$$

where m is the slope and b the intercept specific to a particular functional/basis set combination. These values were determined previously from best fits over 43 molecules in a training set containing diverse organic functionality.⁵

When the appropriate linear correction is applied to the computed ^1H chemical shifts from each of the B3LYP, WP04, and PBE1 methods (Tables 8–10) the accuracy ($|\Delta\delta|_{\text{T}}$) improves slightly for most of the comparisons (cf. Tables 1–3 vs. 8–10; note that the correlation coefficient for linear regression of predicted data on experimental data is unchanged by application of Eqn (1) to the predicted data, so r^2 is not reported in Tables 8–13). Importantly, use of this correction does not diminish the ability of any of the methods to distinguish between diastereomeric pairs.

Table 5. Correlation matrices between IEFPCM/PBE1/6-311+G(2d,p)//IEFPCM/B3LYP/6-31G(d) and experimental ^{13}C NMR chemical shifts^a

	2c^{comp}	2t^{comp}		3c^{comp}	3t^{comp}		4c^{comp}	4t^{comp}
2c^{exp}	0.9975 20.7 (3.0)	0.9899 44.7 (6.4)	3c^{exp}	0.9951 20.2 (2.9)	0.9946 6.6 (0.9)	4c^{exp}	0.9961 20.3 (2.9)	0.9837 38.4 (5.5)
2t^{exp}	0.9937 8.6 (1.2)	0.9971 20.3 (2.9)	3t^{exp}	0.9696 38.3 (5.5)	0.9943 20.5 (2.9)	4t^{exp}	0.9837 10.1 (1.4)	0.9921 18.6 (2.7)

^a Data are reported as r^2 (unitless), $|\Delta\delta|_{\text{T}}$ (ppm, italic), and MUE (ppm, parentheses).

Table 6. Correlation matrices between IEFPCM/WC04/6-311+G(2d,p)//IEFPCM/B3LYP/6-31G(d) and experimental ^{13}C NMR chemical shifts^a

	2c^{comp}	2t^{comp}		3c^{comp}	3t^{comp}		4c^{comp}	4t^{comp}
2c^{exp}	0.9981 14.7 (2.1)	0.9929 27.7 (4.0)	3c^{exp}	0.9987 11.2 (1.6)	0.9855 18.3 (2.6)	4c^{exp}	0.9993 10.5 (1.5)	0.9862 23.3 (3.3)
2t^{exp}	0.9918 21.8 (3.1)	0.9973 14.0 (2.0)	3t^{exp}	0.9858 21.6 (3.1)	0.9990 11.4 (1.6)	4t^{exp}	0.9885 19.0 (2.7)	0.9983 10.9 (1.6)

^a Data are reported as r^2 (unitless), $|\Delta\delta|_{\text{T}}$ (ppm, italic), and MUE (ppm, parentheses).

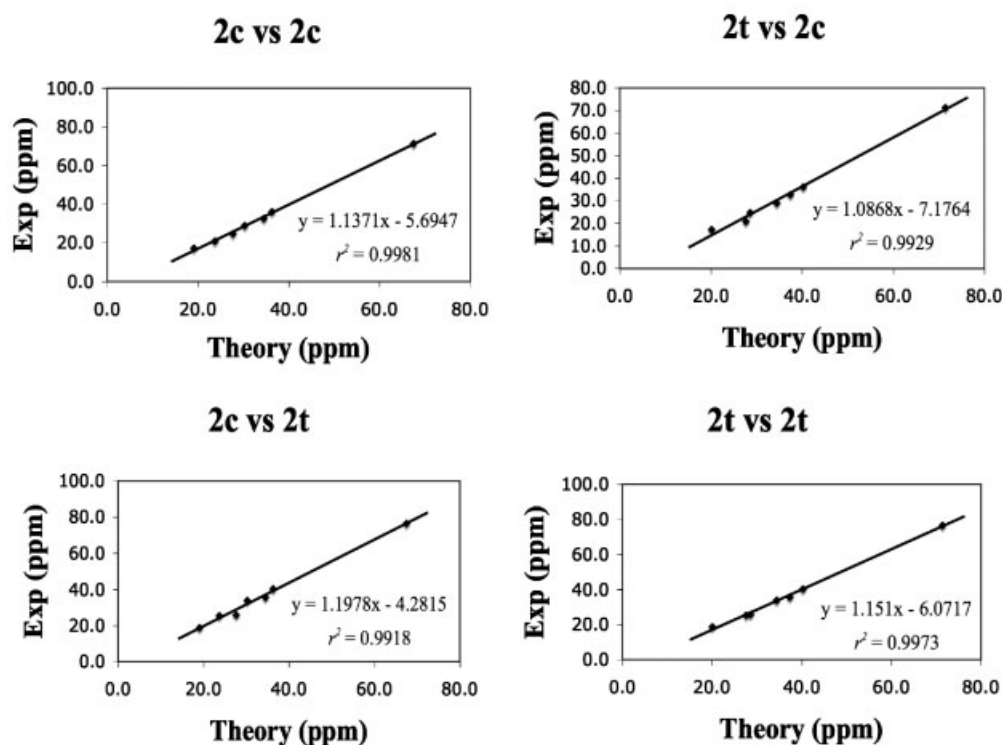


Figure 5. An example (**2c** vs. **2t**) of a regression comparison of theoretical and experimental ^{13}C chemical shift data that form the basis for the statistics in Table 6

Table 7. Slope (m , unitless) and intercept (b , ppm) values for linear correction of chemical shifts predicted from various levels of theory^a

Theory	^{13}C		^1H	
	m	b	m	b
B3LYP	0.9488	-2.1134	0.9333	0.1203
WP04	0.9601	-3.0273	0.9587	0.1127
WC04	1.0032	-0.9647	0.9451	0.1157
PBE1	0.9486	-1.270	0.9169	0.1895

^a For use with IEFPCM/Theory/6-311+G(2d,p)//IEFPCM/B3LYP/6-31G(d). See reference 5

Linear correction also improves the accuracy (MUE) of the computed ^{13}C shifts for each of the B3LYP, WC04, and PBE1 methods (Tables 11–13). In addition, the ability of the B3LYP and PBE1 methods to distinguish between pairs of stereoisomers improves (compare Tables 11 to 4 and 12 to 5), albeit not to perfection. In particular, the B3LYP method still fails for the **3c/t** pair even after application of the appropriate linear correction. The

WC04 method, after correction, continues successfully to distinguish all pairs of stereoisomers (Table 13).

Comparison of the use of ^1H -*versus* ^{13}C -chemical shifts to distinguish stereoisomers

To assess the relative merits of using proton *versus* carbon chemical shifts, we compared the average ratios of the total absolute error values ($|\Delta\delta|_{\text{T}}$. Namely, these ratios for the incorrect to correct pairings of configurations [for linearly corrected hydrogen (Tables 8–10) and carbon (Tables 11–13), and across all of the different protocols] are 5.4 for proton and 2.9 for carbon. Thus, ^1H chemical shifts are about twice as effective in their ability to discriminate the stereochemical differences in these systems as are ^{13}C chemical shifts. This ability may justify the use of hydrogen-based comparisons for compounds structurally related to those studied here. It is true that more often than for proton, ^{13}C NMR

Table 8. Correlation matrices between linearly corrected IEFPCM/B3LYP/6-311+G(2d,p)//IEFPCM/B3LYP/6-31G(d) and experimental ^1H NMR chemical shifts^a

	2c^{corr}	2t^{corr}		3c^{corr}	3t^{corr}		4c^{corr}	4t^{corr}
2c^{exp}	0.66 (0.05)	3.12 (0.24)	3c^{exp}	0.68 (0.05)	3.28 (0.25)	4c^{exp}	0.33 (0.03)	2.94 (0.23)
2t^{exp}	3.29 (0.25)	0.53 (0.04)	3t^{exp}	3.17 (0.24)	0.57 (0.04)	4t^{exp}	3.08 (0.24)	0.42 (0.03)

^a Data are reported as $|\Delta\delta|_{\text{T}}$ (ppm, italic) and MUE (ppm, parentheses).

Table 9. Correlation matrices between computed linearly corrected IEFCM/WP04/6-311+G(2d,p)//IEFCM/B3LYP/6-31G(d) and experimental ^1H NMR chemical shifts^a

	2c^{corr}	2t^{corr}		3c^{corr}	3t^{corr}		4c^{corr}	4t^{corr}
2c^{exp}	0.39 (0.03)	2.50 (0.19)	3c^{exp}	0.88 (0.07)	3.14 (0.24)	4c^{exp}	0.64 (0.05)	2.42 (0.19)
2t^{exp}	3.21 (0.25)	0.79 (0.06)	3t^{exp}	2.64 (0.20)	0.56 (0.04)	4t^{exp}	3.03 (0.23)	0.70 (0.05)

^a Data are reported as $|\Delta\delta|_{\text{T}}$ (ppm, italic), and MUE (ppm, parentheses).**Table 10.** Correlation matrices between linearly corrected IEFCM/PBE1/6-311+G(2d,p)//IEFCM/B3LYP/6-31G(d) and experimental ^1H NMR chemical shifts^a

	2c^{corr}	2t^{corr}		3c^{corr}	3t^{corr}		4c^{corr}	4t^{corr}
2c^{exp}	0.75 (0.06)	3.14 (0.24)	3c^{exp}	0.77 (0.06)	3.11 (0.24)	4c^{exp}	0.40 (0.03)	2.62 (0.20)
2t^{exp}	3.20 (0.25)	0.60 (0.05)	3t^{exp}	3.19 (0.24)	0.46 (0.04)	4t^{exp}	3.10 (0.24)	0.52 (0.04)

^a Data are reported as $|\Delta\delta|_{\text{T}}$ (ppm, italic) and MUE (ppm, parentheses).**Table 11.** Correlation matrices between linearly corrected IEFCM/B3LYP/6-311+G(2d,p)//IEFCM/B3LYP/6-31G(d) and experimental ^{13}C NMR chemical shifts^a

	$2\mathbf{c}^{\text{corr}}$	$2\mathbf{t}^{\text{corr}}$		$3\mathbf{c}^{\text{corr}}$	$3\mathbf{t}^{\text{corr}}$		$4\mathbf{c}^{\text{corr}}$	$4\mathbf{t}^{\text{corr}}$
$2\mathbf{c}^{\text{exp}}$	8.5 (1.2)	29.3 (4.2)	$3\mathbf{c}^{\text{exp}}$	8.0 (1.1)	14.8 (2.1)	$4\mathbf{c}^{\text{exp}}$	8.0 (1.1)	26.6 (3.8)
$2\mathbf{t}^{\text{exp}}$	20.3 (2.9)	7.9 (1.1)	$3\mathbf{t}^{\text{exp}}$	24.5 (3.5)	8.8 (1.3)	$4\mathbf{t}^{\text{exp}}$	20.3 (2.9)	7.2 (1.0)

^a Data are reported as $|\Delta\delta|_{\text{T}}$ (ppm, italic) and MUE (ppm, parentheses).**Table 12.** Correlation matrices between linearly corrected IEFCM/PBE1/6-311+G(2d,p)//IEFCM/B3LYP/6-31G(d) and experimental ^{13}C NMR chemical shifts^a

	$2\mathbf{c}^{\text{corr}}$	$2\mathbf{t}^{\text{corr}}$		$3\mathbf{c}^{\text{corr}}$	$3\mathbf{t}^{\text{corr}}$		$4\mathbf{c}^{\text{corr}}$	$4\mathbf{t}^{\text{corr}}$
$2\mathbf{c}^{\text{exp}}$	5.0 (0.7)	22.7 (3.2)	$3\mathbf{c}^{\text{exp}}$	7.2 (1.0)	20.0 (2.9)	$4\mathbf{c}^{\text{exp}}$	5.0 (0.7)	18.4 (2.6)
$2\mathbf{t}^{\text{exp}}$	25.5 (3.6)	6.1 (0.9)	$3\mathbf{t}^{\text{exp}}$	19.6 (2.8)	6.7 (1.0)	$4\mathbf{t}^{\text{exp}}$	23.8 (3.4)	8.6 (1.2)

^a Data are reported as $|\Delta\delta|_{\text{T}}$ (ppm, italic) and MUE (ppm, parentheses).

spectroscopy gives rise to spectra in which all resonances are uniquely *observable*. However, the following points should not be overlooked: (i) the full set of resonances does not need to have been *observed* in order to apply the methods described here, (ii) with the ever-increasing level of access to higher-field NMR instruments, ever-increasing percentages of proton resonances are routinely *observable* in ^1H NMR spectra, (iii) because of routinely available coupling constant values in ^1H spectra,¹⁵ *assignment* of proton resonances is usually more straightforward than for carbon, and (iv) in order to fully *assign* the carbon resonances, one typically relies upon the use of HMQC and HMBC, through which the

proton shift *assignments*, even for overlapping resonances in the ^1H spectra of complex molecules, are simultaneously revealed. Taken together, these points further argue for the preferential use, if possible, of proton chemical shifts for assigning/distinguishing relative configuration of diastereoisomers.

Comparison of two solvation model cavities

All of the DFT calculations described above were carried out using an all-atom molecular cavity computed from atomic Bondi radii. The sensitivity of the predictions to

Table 13. Correlation matrices between linearly corrected IEFCM/WC04/6-311+G(2d,p)//IEFCM/B3LYP/6-31G(d) and experimental ^{13}C NMR chemical shifts^a

	$2\mathbf{c}^{\text{corr}}$	$2\mathbf{t}^{\text{corr}}$		$3\mathbf{c}^{\text{corr}}$	$3\mathbf{t}^{\text{corr}}$		$4\mathbf{c}^{\text{corr}}$	$4\mathbf{t}^{\text{corr}}$
$2\mathbf{c}^{\text{exp}}$	11.4 (1.6)	23.1 (3.3)	$3\mathbf{c}^{\text{exp}}$	9.0 (1.3)	20.8 (3.0)	$4\mathbf{c}^{\text{exp}}$	6.0 (0.9)	18.5 (2.6)
$2\mathbf{t}^{\text{exp}}$	25.3 (3.6)	11.8 (1.7)	$3\mathbf{t}^{\text{exp}}$	17.1 (2.4)	8.7 (1.2)	$4\mathbf{t}^{\text{exp}}$	21.5 (3.1)	7.6 (1.1)

^a Data are reported as $|\Delta\delta|_{\text{T}}$ (ppm, italic) and MUE (ppm, parentheses).

Table 14. Correlation matrices between IEFPCM/WP04/6-311+G(2d,p)//IEFPCM/B3LYP/6-31G(d) and experimental ^1H NMR chemical shifts^{a,b}

	2c^{comp}	2t^{comp}		3c^{comp}	3t^{comp}		4c^{comp}	4t^{comp}
2c^{exp}	0.9954	0.9077	3c^{exp}	0.9854	0.8565	4c^{exp}	0.9907	0.9341
	<i>0.69 (0.05)</i>	<i>2.46 (0.19)</i>		<i>1.17 (0.09)</i>	<i>3.62 (0.28)</i>		<i>1.25 (0.10)</i>	<i>2.59 (0.20)</i>
2t^{exp}	0.7867	0.9806	3t^{exp}	0.9402	0.9939	4t^{exp}	0.8443	0.9876
	<i>3.69 (0.28)</i>	<i>0.96 (0.07)</i>		<i>2.69 (0.21)</i>	<i>1.07 (0.08)</i>		<i>3.36 (0.26)</i>	<i>1.17 (0.09)</i>

^aData are reported as r^2 (unitless), $|\Delta\delta|_{\text{T}}$ (ppm, italic) and MUE (ppm, parentheses).^bIEFPCM cavities constructed from UA0 radii.

variation of the molecular cavity was assessed by repeating the calculations using a united-atom (UA0) molecular cavity (in this cavity, radii for the heavy atoms are adjusted based on the number of attached hydrogen atoms such that these lighter atoms are fully encompassed by the heavy-atom radii; an advantage of this approach is that some numerical stability is associated with fewer spherical intersections defining the cavity surface). Correlation matrices for theoretical and experimental hydrogen chemical shifts using the UA0 cavity are shown in Table 14. For all stereochemical pairs, the WP04 method using the united-atom cavity continued to be able to distinguish relative configuration with an average difference of 0.1107 for r^2 and 2.02 ppm for the average total absolute error between theory and experiment $|\Delta\delta|_{\text{T}}$. The average MUE of the computations for stereochemical matches using the united-atom cavity (0.080 ppm) was nearly the same as that obtained using the all-atom cavity (0.075 ppm, Table 2) indicating a lack of sensitivity to the nature of the solvation cavity for this method.

The WC04 model was also examined with the united-atom cavity (Table 15). WC04 continues to be

able to distinguish relative configuration for all stereochemical pairs with an average difference of 0.0107 for r^2 and 10.4 ppm for the average total absolute error between theory and experiment $|\Delta\delta|_{\text{T}}$. The average MUEs of the computations using the united-atom and all-atom cavities (Table 6) were 1.75 and 1.73 ppm respectively, indicating that WC04 is not particularly sensitive to this variable.

Error introduced by using only the global minimum energy conformer

Although a complete conformational search is in principle advisable for any organic molecule, one may ask the degree of error introduced by using only a single conformation. The best choice of a single conformation is arguably the global minimum energy conformer. For **2c**, **3t**, and **4c** we examined this point specifically (for the other three stereoisomers, the *trans*-diaxial conformation is so high in energy that it contributes negligibly to the population average).

Data for ^1H and ^{13}C NMR chemical shifts at the WP04 and WC04 level, respectively, are provided in Tables 16

Table 15. Correlation matrices between IEFPCM/WC04/6-311+G(2d,p)//IEFPCM/B3LYP/6-31G(d) and experimental ^{13}C NMR chemical shifts^{a,b}

	2c^{comp}	2t^{comp}		3c^{comp}	3t^{comp}		4c^{comp}	4t^{comp}
2c^{exp}	0.9975	0.9917	3c^{exp}	0.9976	0.9819	4c^{exp}	0.9985	0.9840
	<i>15.2 (2.2)</i>	<i>27.9 (4.0)</i>		<i>10.7 (1.5)</i>	<i>20.1 (2.9)</i>		<i>10.6 (1.5)</i>	<i>22.3 (3.2)</i>
2t^{exp}	0.9897	0.9957	3t^{exp}	0.9862	0.9985	4t^{exp}	0.9874	0.9974
	<i>23.8 (3.4)</i>	<i>15.1 (2.2)</i>		<i>21.0 (3.0)</i>	<i>11.1 (1.6)</i>		<i>20.4 (2.9)</i>	<i>10.3 (1.5)</i>

^{a,b}Data are reported as r^2 (unitless), $|\Delta\delta|_{\text{T}}$ (ppm, italic) and MUE (ppm, parentheses).^dIEFPCM cavities constructed from UA0 radii.**Table 16.** Single conformer correlation matrices between IEFPCM/WP04/6-311+G(2d,p)//IEFPCM/B3LYP/6-31G(d) and experimental ^1H NMR chemical shifts^{a,b}

	2c^{comp}	2t^{comp}		3c^{comp}	3t^{comp}		4c^{comp}	4t^{comp}
2c^{exp}	0.9846	0.9285	3c^{exp}	0.9715	0.8670	4c^{exp}	0.9836	0.9459
	<i>0.95 (0.07)</i>	<i>2.31 (0.18)</i>		<i>1.43 (0.11)</i>	<i>3.55 (0.27)</i>		<i>1.55 (0.12)</i>	<i>2.47 (0.19)</i>
2t^{exp}	0.7611	0.9228	3t^{exp}	0.9515	0.9904	4t^{exp}	0.8411	0.9794
	<i>3.76 (0.29)</i>	<i>2.36 (0.18)</i>		<i>2.60 (0.20)</i>	<i>1.42 (0.11)</i>		<i>3.39 (0.26)</i>	<i>1.26 (0.10)</i>

^{a,b}Data are reported as r^2 (unitless), $|\Delta\delta|_{\text{T}}$ (ppm, italic), and MUE (ppm, parentheses).^aIEFPCM cavities constructed from UA0 radii.

Table 17. Single conformer correlation matrices between IEFPCM/WC04/6-311+G(2d,p)//IEFPCM/B3LYP/6-31G(d) and experimental ^{13}C NMR chemical shifts^{a,b}

	2c^{comp}	2t^{comp}		3c^{comp}	3t^{comp}		4c^{comp}	4t^{comp}
2c^{exp}	0.9988 <i>19.4 (2.8)</i>	0.9904 <i>27.2 (3.9)</i>	3c^{exp}	0.9947 <i>11.1 (1.6)</i>	0.9706 <i>22.1 (3.2)</i>	4c^{exp}	0.9908 <i>13.6 (1.9)</i>	0.9807 <i>21.4 (3.1)</i>
2t^{exp}	0.9728 <i>28.7 (4.1)</i>	0.9920 <i>17.8 (2.5)</i>	3t^{exp}	0.9833 <i>19.8 (2.8)</i>	0.9934 <i>14.2 (2.0)</i>	4t^{exp}	0.9738 <i>22.7 (3.2)</i>	0.9926 <i>10.9 (1.5)</i>

^{a,b} Data are reported as r^2 (unitless), $|\Delta\delta|_{\text{T}}$ (ppm, italic), and MUE (ppm, parentheses).^c IEFPCM cavities constructed from UA0 radii.

and 17. As can be seen in Table 16 for computed ^1H shifts, use of a single conformer *did not prevent* the method from successfully making all stereochemical distinctions. However, accuracy did suffer slightly as is apparent from the average MUE value for stereochemical matches (0.11 ppm, Table 16) as compared to the average MUE obtained using the full conformer complement (0.08 ppm, Table 14). For computed ^{13}C shifts again a larger average MUE for the correct stereochemical matches was obtained using a single isomer (2.1 ppm, Table 17) as compared to those computations using the full conformer complement (1.8 ppm, Table 15).

CONCLUSIONS

Comparison of computed and experimental ^1H and ^{13}C NMR chemical shifts can offer a decisive basis for stereochemical assignment of pairs of diastereoisomers like the *cis*- and *trans*-isomers of 2-, 3-, and 4-methylcyclohexanol. The use of density functionals specifically designed for the prediction of chemical shift data (WP04 and WC04) together with linear correction provides the best results, although standard functionals also do well in most instances. Use of the method based on *proton* shift comparisons is recommended for compounds of this type because it showed better ability to discriminate between stereochemical differences than did the *carbon*-based method.

EXPERIMENTAL METHODS

All compounds were available commercially as mixtures of *cis* and *trans* isomers. Mixtures were purified with silica gel chromatography using 7:3 hexane/ethyl acetate as the eluent. The chromatographic process was monitored using a refractive index detector.

The ^{13}C and ^1H NMR spectra were obtained at ambient temperature in CDCl_3 with chemical shifts determined relative to CDCl_3 (δ 77.23 ppm) for ^{13}C and tetramethylsilane (δ 0.00 ppm) for ^1H spectra. Proton spectra were recorded with acquisition times of 2 s and a spectral width of 8000 Hz; coupling constant values are significant to the nearest 0.25 Hz. A Varian VI-500 MHz NMR instrument was used throughout.

^{13}C NMR shifts were assigned with HMQC and ^1H NMR shifts were assigned using coupling constant analysis and COSY and HMQC experiments. Titration of NMR samples in CDCl_3 with small amounts of benzene- d_6 proved helpful in resolving a few overlapping multiplets. The ^1H and ^{13}C NMR data for **2c/t** thru **4c/t** in CDCl_3 are provided below.

cis-2-Methylcyclohexanol (2c). ^1H NMR (CDCl_3) δ 0.94 (d, 3 H, J = 6.8 Hz, CH_3), 1.25 (m, 1 H, 4a), 1.35 (m, 1 H, 5e), 1.36 (m, 2 H, 3a and 3e), 1.46 (m, 1 H, 6a), 1.55 (m, 2 H, 4e and 5a), 1.60 (m, 1 H, 2a), 1.75 (m, 1 H, 6e), and 3.78 (ddd, 1 H, J = 5.2, 2.7, 2.7 Hz, 1e); ^{13}C NMR (CDCl_3) δ 17.2 (CH_3), 20.9 (C5), 24.7 (C4), 29.0 (C3), 32.7 (C6), 36.1 (C2), and 71.3 (C1).

trans-2-Methylcyclohexanol (2t). ^1H NMR (CDCl_3) δ 0.96 (dddd, 1H, J = 12.9, 12.9, 12.9, 3.3 Hz, 3a), 1.00 (d, 3 H, J = 6.4 Hz, CH_3), 1.18 (dddd, 1H, J = 12.4, 12.4, 12.4, 3.6, 3.6 Hz, 4a), 1.18 (m, 1 H, 6a), 1.25 (m, 2H, 2a and 5a), 1.60 (m, 1 H, 4e), 1.70 (m, 1 H, 3e), 1.72 (m, 1 H, 5e), 1.94 (m, 1 H, 6e), and 3.11 (ddd, 1 H, J = 9.8, 9.8, 4.0 Hz, 1a); ^{13}C NMR δ 18.7 (CH_3), 25.4 (C5), 25.8 (C4), 33.8 (C3), 35.6 (C6), 40.4 (C2), and 76.6 (C1).

cis-3-Methylcyclohexanol (3c). ^1H NMR (CDCl_3) δ 0.76 (dddd, 1H, J = 13.1, 13.1, 11.6, 3.8 Hz, 4a), 0.88 (ddd, 1 H, J = 11.7, 11.7, 11.7 Hz, 2a), 0.92 (d, 3 H, J = 6.6 Hz, CH_3), 1.15 (dddd, 1 H, J = 12.8, 12.8, 10.9, 3.8 Hz, 6a), 1.26 (dddd, 1 H, J = 13.3, 13.3, 13.3, 3.5, 3.5 Hz, 5a), 1.42 (ddddq, 1H, J = 11.8, 11.8, 3.3, 3.3, 6.6 Hz, 3a), 1.74 (dddd, 1H, J = 13.4, 3.4, 3.4, 3.4, 3.4 Hz, 5e), 1.94 (m, 2 H, 2e and 6e), and 3.56 (dddd, 1H, J = 11.0, 11.0, 4.3, 4.3 Hz, 1a); ^{13}C NMR (CDCl_3) δ 22.5 (CH_3), 24.3 (C5), 31.6 (C3), 34.2 (C4), 35.5 (C6), 44.7 (C2), and 70.8 (C1).

trans-3-Methylcyclohexanol (3t). ^1H NMR (CDCl_3) δ 0.89 (d, 3H, J = 6.5 Hz, CH_3), 0.96 (m, 1 H, 4a), 1.23 (ddd, 1 H, J = 13.7, 11.0, 2.9 Hz, 2a), 1.49 (m, 1 H, 6a), 1.51 (m, 1 H, 5e), 1.61 (m, 1 H, 5a), 1.63 (m, 2 H, 4e and 6e), 1.69 (m, 1 H, 2e), 1.83 (ddddq, 1 H, J = 10.4, 10.4, 3.5, 3.5, 6.9 Hz, 3a), and 4.05 (dddd, 1 H, J = 4.4, 4.4, 3.0, 3.0 Hz, 1e); ^{13}C NMR (CDCl_3) δ 20.2 (C5), 22.2 (CH_3), 26.7 (C3), 33.2 (C6), 34.4 (C4), 41.7 (C2), and 67.1 (C1).

cis-4-Methylcyclohexanol (4c). ^1H NMR (CDCl_3) δ 0.92 (d, 3H, J = 6.5 Hz, CH_3), 1.34 (dddd, 2H, J = 14.4, 10.8, 10.8, and 3.6 Hz, 3a and 5a), 1.46 (m, 2H, 3e and 5e), 1.47 (m, 1H, 4a), 1.56 (dddd, 2H, J = 13.9, 11.2, 3.9, 3.0 Hz, 2a and 6a), 1.70 (m, 2 H, 2e and 6e), and 3.94 (tt, 1 H,

$J = 4.9, 3.3$ Hz, 1e); ^{13}C NMR (CDCl_3) δ 21.9 (CH_3), 29.2 (C_3, C_5), 31.4 (C_4), 32.4 (C_2, C_6), and 67.1 (C_1). **trans-4-Methylcyclohexanol (4t)**. ^1H NMR (CDCl_3) δ 0.88 (d, 3H, $J = 6.6$ Hz, CH_3), 0.97 (dddd, 2H, $J = 13.4, 13.4, 11.6, 3.3$ Hz, 3a and 5a), 1.25 (dddd, 2H, $J = 13.4, 12.4, 11.0, 3.7$ Hz, 2a and 6a), 1.33 (ttq, 1H, $J = 11.9, 3.8, 6.9$ Hz, 4a), 1.70 (m, 2H, 3e and 5e), 1.93 (m, 2H, 2e and 6e), and 3.53 (tt, 1H, $J = 10.9, 4.3$ Hz, 1a); ^{13}C NMR (CDCl_3) δ 22.1 (CH_3), 31.9 (C_4), 33.5 (C_3, C_5), 35.7 (C_2, C_6), and 71.0 (C_1).

Acknowledgements

This work was supported in part by the National Science Foundation (CJC, CHE-0203346) and the National Institutes of Health (TRH, CA76497). Supporting Information Available: Copies of 1D ^1H and ^{13}C NMR spectra, computed geometries and energies, and computed ^1H and ^{13}C chemical shifts for each of **2c/t** thru **4c/t** (57 pages).

REFERENCES

- (a) Kobayashi Y, Lee J, Tezuka K, Kishi Y. *Org. Lett.* 1999; **1**: 2177–2180; (b) Seike H, Ghosh I, Kishi Y. *Org. Lett.* 2006; **8**: ASAP (and references therein).
- (a) Bringmann G, Schlauer J, Rischer H, Wohlfarth M, Muehlbacher J, Buske A, Porzel A, Schmidt J, Adam G. *Tetrahedron* 2000; **56**: 3691–3695; (b) Kisiel W, Zielinska K. *Phytochemistry* 2001; **57**: 523–527; (c) Monica CD, Randazzo A, Bifulco G, Cimino P, Aquino M, Izzo I, De Riccardis F, Gomez-Paloma L. *Tetrahedron Lett.* 2002; **43**: 5707–5710; (d) Wipf P, Kerekes AD. *J. Nat. Prod.* 2003; **66**: 716–718.
- Cramer CJ. *Essentials of Computational Chemistry: Theories and Models*, (2nd edn). John Wiley & Sons: Chichester, 2004.
- (a) Stahl M, Schopfer U, Frenking G, Hoffmann RW. *J. Org. Chem.* 1996; **61**: 8083–8088; (b) Clark AJ, Ellard JM. *Tetrahedron Lett.* 1998; **39**: 6033–6036; (c) Sebag AB, Forsyth DA, Plante MA. *J. Org. Chem.* 2001; **66**: 7967–7973; (d) Barone G, Duca D, Silvestri A, Gomez-Paloma L, Riccio R, Bifulco G. *Chem. Eur. J.* 2002; **8**(14): 3233–3239; (e) Barone G, Duca D, Silvestri A, Gomez-Paloma L, Riccio R, Bifulco G. *Chem. Eur. J.* 2002; **8**(14): 3240–3245; (f) Colombo D, Ferraboschi P, Ronchetti F, Toma L. *Magn. Reson. Chem.* 2002; **40**: 581–588; (g) Giesen DJ, Zumbulyadis N. *Phys. Chem. Chem. Phys.* 2002; **4**: 5498–5507; (h) Migda W, Rys B. *Magn. Reson. Chem.* 2004; **42**: 459–466.
- Wiitala KW, Hoye TR, Cramer CJ. *J. Chem. Theor. Comput.* 2006; **2**: 1085–1092.
- (a) Becke AD. *Phys. Rev. A* 1988; **38**: 3098–3100; (b) Lee C, Yang W, Parr RG. *Phys. Rev. B* 1988; **37**: 785–789; (c) Becke AD. *J. Chem. Phys.* 1993; **98**: 5648–5652; (d) Stephens PJ, Devlin FJ, Chabalowski CF, Frisch MJ. *J. Phys. Chem.* 1994; **98**: 11623–11627.
- Hehre WJ, Radom L, Schleyer PR, Pople JA. *Ab Initio Molecular Orbital Theory*, Wiley: New York, 1986.
- (a) Mennucci B, Tomasi J. *J. Chem. Phys.* 1997; **106**: 5151–5158; (b) Barone V, Cossi M, Tomasi J. *Chem. Phys. Lett.* 1997; **107**: 3210–3221; (c) Mennucci B, Cancès E, Tomasi J. *J. Phys. Chem. B* 1997; **101**: 10506–10517; (d) Tomasi J, Mennucci B, Cancès E. *J. Mol. Struct. (Theochem)* 1999; **464**: 211–226.
- Barone V, Cossi M, Tomasi J. *J. Chem. Phys.* 1997; **107**: 3210–3220.
- Bondi A. *J. Phys. Chem.* 1964; **68**: 441–451.
- (a) Perdew JP. In *Electronic Structure '91*, Ziesche P, Eschrig H (eds). Akademie Verlag: Berlin, 1991; 11–20; (b) Perdew J, Wang Y. *Phys. Rev. B* 1992; **45**: 13244–13249.
- Frisch MJ, Trucks GW, Schlegel HB, Scuseria GE, Robb MA, Cheeseman JR, Montgomery JA, Jr., Vreven T, Kudin KN, Burant JC, Millam JM, Iyengar SS, Tomasi J, Barone V, Mennucci B, Cossi M, Scalmani G, Rega N, Petersson GA, Nakatsuji H, Hada M, Ehara M, Toyota K, Fukuda R, Hasegawa J, Ishida M, Nakajima T, Honda Y, Kitao O, Nakai H, Klene M, Li X, Knox JE, Hratchian HP, Cross JB, Bakken V, Adamo C, Jaramillo J, Gomperts R, Stratmann RE, Yazyev O, Austin AJ, Cammi R, Pomelli C, Ochterski JW, Ayala PY, Morokuma K, Voth GA, Salvador P, Dannenberg JJ, Zakrzewski VG, Dapprich S, Daniels AD, Strain MC, Farkas O, Malick DK, Rabuck AD, Raghavachari K, Foresman JB, Ortiz JV, Cui Q, Baboul AG, Clifford S, Cioslowski J, Stefanov BB, Liu G, Liashenko A, Piskorz P, Komaromi I, Martin RL, Fox DJ, Keith T, Al-Laham MA, Peng CY, Nanayakkara A, Challacombe M, Gill PMW, Johnson B, Chen W, Wong MW, Gonzalez C, Pople JA. *Gaussian03RevisionB05* GaussianIncWallingfordCT 2004.
- Subbotin OA, Sergeyev NM, Chlopkov VN, Nikishova NG, Bundel YG. *Org. Magn. Res.* 1980; **13**: 259–262.
- (a) Wang B, Hinton JF, Pulay P. *J. Comput. Chem.* 2002; **23**: 492–497; (b) Wang B, Fleischer U, Hinton JF, Pulay P. *J. Comput. Chem.* 2001; **22**: 1887–1895; (c) Giesen DJ, Zumbulyadis N. *Phys. Chem. Chem. Phys.* 2002; **4**: 5498–5507; (d) Sebag AB, Forsyth DA, Plante MA. *J. Org. Chem.* 2001; **66**: 7967–7973; (e) Rablen PR, Pearlman SA, Finkbiner J. *J. Phys. Chem. A* 1999; **103**: 7357–7363.
- (a) Hoye TR, Zhao H. *J. Org. Chem.* 2002; **67**: 4014–4016; (b) Hoye TR, Hanson PR, Vyvyan JR. *J. Org. Chem.* 1994; **59**: 4096–4103.